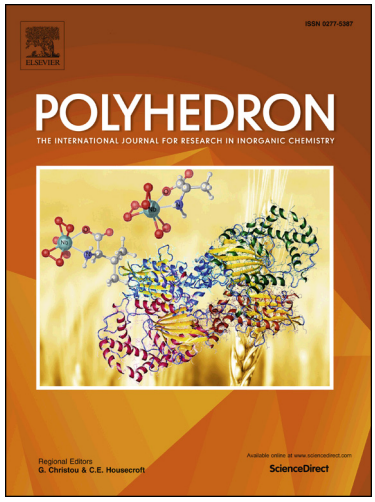

Four homo- and hetero-bismetallic 3d/3d-2s complexes constructed from a naphthalenediol-based acyclic bis(salamo)-type tetraoxime ligand

Jing Hao, Li-Long Li, Jin-Tong Zhang, Sunday Folaranmi Akogun, Li Wang, Wen-Kui Dong

PII: S0277-5387(17)30418-7
DOI: http://dx.doi.org/10.1016/j.poly.2017.05.060
Reference: POLY 12681

To appear in: *Polyhedron*

Received Date: 25 March 2017
Revised Date: 16 May 2017
Accepted Date: 18 May 2017

Please cite this article as: J. Hao, L-L. Li, J-T. Zhang, S. Folaranmi Akogun, L. Wang, W-K. Dong, Four homo- and hetero-bismetallic 3d/3d-2s complexes constructed from a naphthalenediol-based acyclic bis(salamo)-type tetraoxime ligand, *Polyhedron* (2017), doi: http://dx.doi.org/10.1016/j.poly.2017.05.060

Four homo- and hetero-bismetallic 3d/3d-2s complexes constructed from a naphthalenediol-based acyclic bis(salamo)-type tetraoxime ligand

Jing Hao, Li-Long Li, Jin-Tong Zhang, Sunday Folaranmi Akogun, Li Wang, Wen-Kui Dong*

School of Chemical and Biological Engineering, Lanzhou Jiaotong University, Lanzhou, Gansu 730070, PR China

ABSTRACT

The homo/heterotrinuclear metal(II) complexes $[Zn_3(L)(OAc)_2(CH_3OH)_2]\cdot 3CHCl_3$ (**1**), $[Zn_2(L)Ca(OAc)_2]\cdot CHCl_3$ (**2**), $[Zn_2(L)Sr(OAc)_2]$ (**3**) and $[Zn_2Ba(L)(OAc)_2(CH_3OH)]\cdot CH_3OH\cdot CHCl_3$ (**4**), with a novel acyclic bis(salamo)-type tetraoxime ligand H_4L, were synthesized and characterized by elemental analyses, IR, UV-Vis and fluorescence spectra. UV-Vis titrations clearly show that complexation of H_4L with Zn(II) ions affords a stoichiometric ratio of 3:1 (M:L) in a cooperative fashion. Complexes **2**, **3** and **4** can acquire by the substitution reactions of complex **1** with 1 equivalent of $M(OAc)_2$ (M^{2+} = Ca^{2+}, Sr^{2+} or Ba^{2+}). The crystal structures of complexes **1**-**4** have been determined by single-crystal X-ray diffraction. The coordinating ability of the $[Zn_3(L)]^{2+}$ units may be utilized as a cation recognition phenomenon.

Keywords: Acyclic bis(salamo) ligand; Heterobismetallic 3d-2s complex; UV-Vis titration; Crystal structure; Fluorescence property

1. Introduction

Various kinds of salen-type ligands, used for synthesizing functional metal complexe,s have been synthesized by chemical modification of aldehydes or diamines, which are versatile and important compounds [1-3]. Many salen-type metal complexes have already been developed to study their structures, reactivities or fundamental physical properties [4,5]. Polynuclear metal complexes with a variety of interesting structures, such as

* Corresponding authors.
E-mail: dongwk@126.com*; Tel: +86 931 4938703*
† CCDC reference numbers 1424752 (for **1**), 1424753 (for **2**), 1424754 (for **3**) and 1424755 (for **4**).

metallamacrocycles [6], have unique properties and functions like magnetic properties [7], catalytic activity [8], guest recognition [9] and so on. In particular, heteronuclear complexes bearing 3d and 4f transition metals are interesting and important because magnetic superexchange interactions between the bridged metal atoms may exist in the complexes, which can also be used in guest recognition [10]. Simultaneous and synergistic non-covalent interactions result in strong and specific host-guest binding phenomena, except some which are weak [11]. Such a metal-containing ionophore is expected to show an interaction between the guest cations and the metal complex moieties, leading to various kinds of functional host-guest systems [12]. In this paper, using the recognition of metal atoms by the ligand H_4L, on the basis of complex **1**, complexes **2**, **3** and **4** were subjected to UV-Vis titration and fluorescence titration experiments.

A variety of acyclic and cyclic ligands with two kinds of sites have also been designed to synthesize such a heteronuclear complex [13]. At the beginning, preparing the complexes was mostly restricted by the stepwise reactions using a readily available mononuclear complex, which can be regarded as an "addition reaction". However, the preparation of heteronuclear complexes has now been developed, for instance, the metal that initially bonds to one site of some ligands migrates to another site during the second metalation step [14]. Furthermore, metal exchange between two "coordination-position isomers" has also been reported [15,16]. In this context, we used a new method to synthesize $(3d)_2(2s)$ trinuclear complexes, which could be regarded as a "substitution reaction". A $(3d)_3$ homotrinuclear complex prepared with three Zn(II) ions and the acyclic bis(salamo) ligand H_4L, having two salen-type chelating moieties [17], undergoes exclusive and quantitative transmetalation of the central 3d metal ion with a 2s metal ion.

Herein, following our previous studies on the synthesis, structural characterization and optical properties of 3d or 3d–4f salamo-type complexes [18], we report the cooperative formation of trinuclear complexes by the metalation of the bis(salamo) ligand H_4L. The homotrinuclear complex with the central cavity surrounded by six oxygen atoms is expected to have a high affinity toward metal cations, since the donor atoms are arranged in a cyclic fashion and are negatively charged. Through the "substitution reaction", the homotrinuclear complex **1** could be effectively transformed into the heterotrinuclear complexes **2**, **3** and **4**.

2. Experimental

2.1. Materials and instruments

2-Hydroxy-3-methoxybenzaldehyde (99%), methyl trioctyl ammonium chloride (90%), pyridiniumchlorochromate (98%) and borontribromide (99.9%) were purchased from Alfa Aesar. Hydrobromic acid 33wt% solution in acetic acid was purchased from J&K Scientific Ltd. The other reagents and solvents were purchased from Shanghai Darui Chemical Fine Chemicals Company. All chemicals were of analytical grade and used without further purification. C, H and N analyses were obtained using a GmbH VarioEL V3.00 automatic elemental analysis instrument. Elemental analyses for the metals were detected with an IRIS ER/S-WP–1 ICP atomic emission spectrometer. IR spectra were recorded on a VERTEX70 FT-IR spectrophotometer, with the samples prepared as KBr (500–4000 cm^{-1}) pellets. UV-Vis absorption spectra were recorded on a Shimadzu UV-2550 spectrometer. ^1H NMR spectra were determined with a German Bruker AVANCE DRX-400 spectrometer. Fluorescent spectra were taken on a LS-55 fluorescence photometer. X-ray single crystal structure determinations were carried out on a Bruker Smart Apex CCD diffractometer. Melting points were obtained with the use of an X4 microscopic melting point apparatus made from the Beijing Taike Instrument Limited Company and were uncorrected.

2.2. Synthesis of the ligand H_4L

The ligand H_4L was obtained by the reaction of 2,3-dihydroxynaph-thalene-1,4-dicarbaldehyde with 2-[*O*-(1-ethyloxyamide)]oxime-6-methoxyphenol, according to the literature [19]. The ^1H NMR spectrum in $CDCl_3$ (Fig. 1) showed signals at δ 11.03 and 9.82 ppm, which could be assigned to the OH protons. However, there were obvious signals at δ 9.14 and 8.29 ppm for the salicylaldimine CH=N protons. The δ 6.68-7.97 ppm peaks could be assigned to the H protons of the naphthalene and benzene rings.

The ligand H_4L is remarkably soluble in chloroform, DMF and DMSO, but only slightly soluble in methanol, ethanol, acetone and ethyl acetate. Its corresponding complexes are stable in air. The reaction steps involved in the synthesis of the bis(salamo)-type tetraoxime ligand (H_4L) are shown in Scheme 1.

Scheme 1. Synthetic route to the bis(salamo)-type tetraoxime ligand H_4L.

*2.3. Synthesis of complexes **1**, **2**, **3** and **4***

*2.3.1. Synthesis of complex **1***

A solution of $Zn(OAc)_2{\cdot}2H_2O$ (6.58 mg, 0.03 mmol) in methanol (3 mL) was added to a solution of the ligand H_4L (6.32 mg, 0.01 mmol) in chloroform (3 mL) at room temperature. The color of the solution immediately turned yellow. The mixture was filtered and the filtrate was allowed to stand at room temperature for about four weeks. The solvent was partially evaporated and several yellow prismatic single crystals were obtained. Yield: 5.62 mg (41.2%). *Anal*. Calc. for $C_{41}H_{45}Cl_9N_4O_{16}Zn_3$: C, 36.07; H, 3.32; N, 4.10. Found: C, 35.96; H, 3.40; N, 3.97%. IR (KBr; cm^{-1}): 1604 [ν(C=N)], 1245 [ν(Ar-O)], 3392 [ν(O–H)]. UV-Vis [in chloroform/methanol (1:1)], λ_{max} (nm) [3.3×10^{-5} M]: 280, 370, 396, 416.

2.3.2. Syntheses of the heterotrinuclear complexes

A solution of $Zn(OAc)_2{\cdot}2H_2O$ (6.58 mg, 0.03 mmol) in methanol (1 mL) and $Ca(OAc)_2$ (1.58 mg, 0.01 mmol) in water/methanol (1:3, 2 mL) were added to a solution of H_4L (6.32 mg, 0.01 mmol) in chloroform (3 mL), and the resulting solution was concentrated to dryness. The solid was redissolved in chloroform/methanol (1:1, 6 mL). The mixture was filtered and the filtrate was allowed to stand at room temperature for several weeks, giving yellow crystals of complex **2**. Complexes **3** and **4** were prepared by a similar procedure as for complex **2**.

Complex **2**, yellow crystals, Yield: 4.73 mg (45.6%). *Anal*. Calc. for $C_{37}H_{35}CaCl_3N_4O_{14}Zn_2$: C, 42.86; H, 3.40; N, 5.40. Found: C, 42.79; H, 3.23; N, 5.27%. IR (KBr; cm^{-1}): 1610 [ν(C=N)], 1238 [ν(Ar–O)]. UV-Vis [in chloroform/methanol (1:1)], λ_{max} (nm) [3.3×10^{-5} M)]: 280, 370, 396, 416.

Complex **3**, yellow crystals, Yield: 3.31 mg (34.3%). *Anal*. Calc. for $C_{36}H_{34}N_4O_{14}SrZn_2$: C, 44.80; H, 3.55; N, 5.81. Found: C, 44.73; H, 3.62; N, 5.75%. IR (KBr; cm^{-1}): 1610 [ν(C=N)], 1235 [ν(Ar-O)]. UV-Vis [in chloroform/methanol (1:1)], λ_{max} (nm) [3.3×10^{-5} M)]: 280, 370, 396, 416.

Complex **4**, yellow crystals, Yield: 3.01 mg (25.1%). *Anal*. Calc. for $C_{39}H_{43}BaCl_3N_4O_{16}Zn_2$: C, 39.09; H, 3.62; N, 4.68. Found: C, 39.21; H, 3.72; N, 4.62%. IR (KBr; cm^{-1}): 1610 [ν(C=N)],

1235 [ν(Ar-O)], 3434 [ν(O-H)]. UV-Vis [chloroform/methanol (1:1)], [3.3×10^{-5} M)] λ_{max} (nm): 280, 370, 396, 416.

2.4. X-ray crystal structure determination

Intensity data for complexes **1**, **2** and **3** were collected on a SuperNova (Dual, Cu at zero, Eos) diffractometer with Mo K_α radiation (λ = 0.71073 Å) at 173.00(10), 293(2) and 294.29(10) K, respectively, while intensity data for complex **4** was collected on a Bruker Smart 1000 CCD area detector with Mo K_α radiation (λ = 0.71073 Å) at 291.73(10) K. Reflection data were corrected for Lorentz and polarization factors and for absorption using the multi-scan method. The structures were solved by using the program SHELXL-97 and Fourier difference techniques, and refined by the full-matrix least-squares method on F^2. All hydrogen atoms were added in calculated positions. The crystallographic data are summarized in Table 1.

Table 1 Crystallographic data and refinement parameters for the complexes **1**, **2**, **3** and **4**.

3. Results and discussion

3.1. Crystal structures

Complex **1** was synthesized by the reaction of the ligand H_4L with 3 equivalents of the Zn^{2+} ion. Complexes **2**, **3** and **4** were prepared by the reactions of complex **1** with 1 equivalent of $M(OAc)_2$ (M^{2+} = Ca^{2+}, Sr^{2+} or Ba^{2+}). Complex **1** dissolves in DMF and chloroform, but is only slightly soluble in methanol. Complexes **2**, **3** and **4** have similar solubility. The heterotrinuclear complexes **2**-**4** were synthesized by using Ca^{2+}, Sr^{2+} and Ba^{2+} ions to replace the central Zn^{2+} ion of complex **1**, $[Zn_3(L)]^{2+}$ (Scheme 2). All the structures of the complexes were determined by single-crystal X-ray diffraction. Selected bond lengths and bond angles are listed in Table S1.

Scheme 2. Formation of the trinuclear complexes **L**·M_3 from the bis(salamo) ligand H_4L and ion recognition based on metal exchange.

*3.1.1. Structure of complex **1***

The crystal structure and atom numbering of complex **1** are shown in Fig. 2. Complex **1** crystallizes in the monoclinic system, space group $P2_1/n$. X-ray crystallography clearly shows the formation of complex **1**, which was isolated as yellow crystals. Interestingly, the formation

process of complex **1** was highly cooperative. In the crystal structure of complex **1**, two acetate ions bridge the trinuclear Zn^{2+} ions in a μ_2-fashion, which probably contributes to the cooperative formation of complex **1**. The Zn1 and Zn2 atoms are both five-coordinated with distorted trigonal bipyramidal geometries, which were deduced by calculating the τ values, where τ_1 = 0.8227 and τ_2 = 0.6943 [20]. The Zn3 atom is six-coordinated, with a distorted octahedral geometry. The distances between the Zn3 atom and the coordinated oxygen atoms range from 2.02 to 2.19 Å. The Zn3 atom is located in the cavity that consists of six oxygen atoms, where four oxygen atoms are phenoxy oxygen atoms and the other two oxygen atoms are from the methoxy groups.

Fig. 2. X-ray crystal structure of complex **1**.

In the crystal structure of complex **1**, there is a significant intermolecular hydrogen bond (C10-H10A···O12) between the complex **1** units, which links the units together efficiently to form a 1D chain supra-molecular structure along the *b* axis (Fig. S1).

As a result, metalation of the bis(salamo) ligand H_4L affords the trinuclear complex $[Zn_3(L)]^{2+}$ instead of the dinuclear complex $[Zn_2(L)]$. Complex **1** was not the desired product because its cavity is occupied by an additional Zn^{2+} ion,as is evident from the crystal structure. However, the size of the cavity seems to be too large to fit in the central Zn^{2+} ion because only two donor atoms coordinate to the central Zn^{2+} ion in the crystal structure. Thus, this structure suggests that the central Zn^{2+} ion should be replaced by a metal ion with a suitable size for the cavity. Thus the 2s ions having a suitable radius are utilized in a "substitution reaction" to prepare heteronuclear complexes.

*3.1.2. Structure of complex **2***

The crystal structure and atom numbering of complex **2** is shown in Fig. 3(a). Complex **2** crystallizes in the triclinic, space group $\bar{P}1$. In complex **2**, The Zn1 and Zn2 atoms are located in the N_2O_2 salamo moieties, two acetate ions bridge the Zn^{2+} ions and the Ca^{2+} ion in a μ_2-fashion. The Zn1 and Zn2 atoms are both five-coordinated with tetragonal pyramidal geometries, which were deduced by calculating the τ values, where τ_3 = 0.3335 and τ_4 = 0.2287, for the Zn1 and Zn2 atoms, respectively [20]. The Ca1 atom is eight-coordinated with the a square antiprismatic geometry, replacing the central Zn^{2+} ion

of complex **1**. Here, all the six oxygen atoms of the [LZn_2] moiety coordinate nicely to the Ca1 atom. Complex **2** has weak coordination with the methoxy groups, deduced by analyzing the distance between the Ca1 atom and the oxygen atoms of the methoxy groups. The distances between the Ca1 atom and the four phenoxy oxygen atoms of the salamo moieties range from 2.365(4) to 2.432(3) Å, which are obviously shorter than the bond distances to the methoxy groups (Ca1-O1 2.678(3) Å, Ca1-O10 2.643(3) Å). This fact clearly shows that the coordination bonds of the former are stronger than those of the later. Intermolecular hydrogen bonds (C7-H7···O11, C24-H24···O13) between complex **2** units obviously link the units together efficiently, and the interlinked units eventually form a 1D chain supra-molecular structure, which is very similar to complex **1** (Fig. S2).

In summary, the stable complex **2** is obtained by the substitution reaction of the Ca^{2+} ion with complex **1**, where the space group and geometries of the Zn1 and Zn2 atoms are all different from that of complex **1**. Compared with the oxygen atoms of the methoxy groups, Ca1 has a strong coordination with the phenoxy oxygen atoms, which probably results from the electrostatic interaction.

Fig. 3. X-ray crystal structures of the heterotrinuclear complexes: (a) complex **2**, (b) complex **3**, (c) complex **4**.

3.1.3. Structure of complex 3

The crystal structure and atom numbering of complex **3** is shown in Fig. 3(b). Complex **3** crystallizes in the triclinic system, space group $\bar{P}1$. The Zn^{2+} ions of complex **3** have similar coordination environments and coordination geometries, with the τ values τ_5 = 0.4233 (Zn1) and τ_6 = 0.5087 (Zn2) [20]. Both zinc atoms are five-coordinated with tetragonal pyramidal (Zn1) and trigonal bipyramidal (Zn2) geometries. The Sr1 atom is eight-coordinated with a square antiprismatic geometry, which is similar to the Ca1 atom in complex **2**. The distances between the Sr1 atom and the four phenoxy oxygen atoms of the coordinated salamo moieties range from 2.501(4) to 2.569(5) Å, which are obviously shorter than the bond distances to the methoxy groups (Sr1-O1 2.645(5) Å, Sr1-O10 2.735(4) Å). The Sr-O bonds in complex **3** experience the same coordination environment as the Ca-O bonds in complex **2**, however, these bonds are obviously longer than the corresponding Ca-O bond lengths found in complex **2**.

In the crystal structure of complex **3** there are significant intermolecular hydrogen bonds (C16-H16···O3, C24-H24···O11) and C-H···π interactions (C8-H8B···*Cg*6 (C1-C6), C22-H22A···*Cg*5 (C11-C20)). Here, complex **3** units are interlinked by the intermolecular hydrogen bonds and C-H···π interactions into a 2D supra-molecular structure (Fig. S3).

*3.1.4. Structure of complex **4***

The crystal structure and atom numbering of complex **4** is shown in Fig. 3(c). Complex **4** crystallizes in the triclinic system, space group $\bar{P}1$, which is the same as complexes **2** and **3**. The Zn^{2+} ions of complex **4** are both five-coordinated with tetragonal pyramidal geometries, derived from the τ values of τ_7 = 0.4688 (Zn1) and τ_8 = 0.4263 (Zn2) [20]. In this complex the Ba1 atom is nine-coordinated with a single square antiprismatic geometry, which is different from the Ca1 and Sr1 atoms in complexes **2** and **3** because of the coordination of a methanol molecule. The distances between the Ba1 atom and the four phenoxy oxygen atoms of the salamo moieties range from 2.706(4) to 2.814(4) Å, which are obviously shorter than the bond distances to the methoxy groups (Ba1-O1 2.973(5) Å, Ba1-O10 2.955(4) Å). The same situation was also observed in complexes **2** and **3**.

In the crystal structure of complex **4**, because of the presence of methanol molecules, there are more significant intermolecular hydrogen bonds (C23-H23A···O14, O15-H15···O16 and O16-H16A···O13) and C-H···π interactions (C21-H21···*Cg*6 (C11-C12-C17-C18-C19-C20) and C14-H14···*Cg*8 (C25-C30)). Here, complex **4** units are interlinked by the intermolecular hydrogen bond and C-H···π interactions into a 2D supra-molecular structure along the *bc* plane (Fig. S4).

Therefore, the final formed geometries of the Zn1 and Zn2 atoms are both square pyramids, whilst the Ca1 and Sr1 atoms both display square antiprismatic geometries. The Ba1 atom is larger than the Ca1 and Sr1 atoms, so the coordination of the Ba1 atom with a methanol molecule makes the structure more stable. The resulting geometry of the Ba1 atom is a single square antiprism. The coordination bonds of the Ca1 atom with the phenoxy oxygen atoms are obviously shorter than the Ca1 atom with methoxy groups in complex **2**, with complexes **3** and **4** showing the same experimental phenomena. It can be seen that with the increase of the cation radius, the coordination bonds of the central cation are stronger. This fact suggests that the charge of the central cation and the size-fit principle (between the cavity and the central metal cation) are

significant factors which affect the cation-binding ability of complex **1**.

3.2. IR spectra

The IR spectra of the ligand H_4L and its corresponding complexes exhibit various bands in the region 4000-400 cm^{-1}. The most important bands are given in Table S2. The spectrum of the ligand shows an O-H stretching band at 3172 cm^{-1} that belongs to phenolic hydroxyl group, whereas complex **1** shows a band at 3392 cm^{-1} that belongs to the coordinated methanol molecules. The band is shifted by 220 cm^{-1} in complex **1** compared to ligand H_4L, probably resulting from the powerful intramolecular hydrogen bonds in the ligand. The free ligand exhibits characteristic C=N and Ar-O stretching bands at 1607 and 1250 cm^{-1}, respectively. Those bands are shifted by 3-5 cm^{-1} in complex **1**. This lowering of energy results from the Zn-N and Zn-O interactions upon complexation, which is similar to previously reported Zn(II) complexes [21]. Compared with complex **1**, the C=N and Ar-O stretching bands belonging to the heterotrinuclear complexes are shifted by 3 and 7 cm^{-1}, respectively. Meanwhile, the O-H stretching band disappeared in complexes **2** and **3**. The O-H stretching band at 3434 cm^{-1}, attributed to the methanol molecules of complex **4**, is shifted by 42 cm^{-1}. These facts are due to the replacement of the central Zn^{2+} ion by the M^{2+} ions and the formation of new M-O coordination bond. The above facts are consistent with the results determined by X-ray diffraction.

3.3. UV-Vis absorption spectra

In the UV-Vis titration experiment of complex **1**, the color of the ligand solution in chloroform/methanol (1:1) gradually changed from colorless to yellow upon addition of a solution of Zn(II) acetate. The free ligand H_4L shows four strong absorption bands at 269, 343, 360 and 378 nm. However, complex **1** shows four absorption bands at 280, 370, 396 and 416 nm, which are shifted by 11, 27, 36 and 38 nm, respectively. The red-shift phenomena is due to the coordination of the ligand H_4L with the Zn^{2+} ion. In the case of complex **1**, although the ligand H_4L has two salamo chelate moieties, the spectroscopic titration clearly indicates the formation of a 3:1 homotrinuclear Zn(II) complex. The exclusive and cooperative formation of a 3:1 homotrinuclear Zn(II) complex was indicated by the spectral changes, in which the absorbance of the solution hardly changed after Zn^{2+} was added up to 3 equivalents, and the isosbestic points at 274, 308 and 367 nm were observed (Fig. 4).

Fig. 4. (a) UV-Vis spectral changes of H_4L (1.6×10^{-5} M) on addition of $Zn(OAc)_2$ (1.05×10^{-2} M) ($CHCl_3/CH_3OH$ (1:1); (b) UV-Vis spectral changes of complex **1** on addition of $Ca(OAc)_2$ ($[[Zn_3(L)]^{2+}] = 3.3 \times 10^{-5}$ M) (the amount of metal salt added to the ligand H_4L each time was 2 μL)

In the UV-Vis titration experiment of complex **2**, the color of the solution of complex **1** in chloroform/methanol (1:1) changed inconspicuously when a solution of Ca^{2+} ions was added. In the titration experiment, there were neither red-shift nor blue-shift phenomena, except for changes in absorbance, and the absorbance of the solution hardly changed after the Ca^{2+} ion was added up to 1 equivalent. The spectroscopic titration clearly indicates that the ratio of the reaction stoichiometry is 1:1 (Fig. 4). Similar changes were also observed for complexes **3** and **4** (Fig. S5), thus giving the same results.

3.4. Fluorescence tests

The excitation and emission spectra of complex **1** are shown in Fig. 5. The excitation spectrum (435 nm) in a chloroform and methanol solution (1:1) is detected at the same intensity as the corresponding emission spectrum (501 nm) at room temperature. The emission spectrum excited at 435 nm exhibits broad visible luminescence in the range 450 to 650 nm. Since the conjugate system of a naphthalene ring is larger than that of a benzene ring, their optical properties are better than the reported Zn(II) complexes with benzene [22].

Fig. 5. The excitation and emission spectra of complex **1 (**$CHCl_3/CH_3OH$ = 1:1, *v*/*v*, λ_{ex} = 435).

The excitation and emission spectra of complex **2** at room temperature are shown in Fig. 6. Complex **2** shows an intense photoluminescence with a maximum emission at *ca*. 500 nm upon excitation at 429 nm. Upon excitation at 438 and 440 nm, complexes **3** and **4** respectively show maximum emissions at *ca*. 502 and 503 nm, the emission spectra are shown in Fig. 7 and Fig. 8. Compared with complex **1**, strong fluorescence intensities of the heterotrinuclear complexes are observed, indicating that the fluorescent characteristic has been influenced by the introduction of

the alkaline earth metal ions. Among the three heterotrinuclear complexes, the fluorescence intensity of complex **2** is the strongest, while the lowest is observed for complex **4**. It is obvious that enhancement in the fluorescence intensities show declining trend from complex **2** to **4**. Meanwhile, the maximum emissions of the heterotrinuclear complexes have subtle differences, the maximum wavelength shifts from 500 to 503 nm. Differences in the radii of the alkaline earth metal ions may be the main reason for the diverse fluorescence enhancement and peak wavelength variation.

Fig. 6. (a) The excitation and emission spectra of complex **2** (5.0×10^{-5} M) ($CHCl_3/CH_3OH$ = 1:1, *v*/*v*, λ_{ex} = 429 nm). (b) Fluorescence spectral changes of complex **1** by the addition of $Ca(OAc)_2$ (5.0×10^{-3} M) ($CHCl_3/CH_3OH$ (1:1), [complex **1**] = 5.0×10^{-5} M, λ_{ex} = 429) (The amount of $Ca(OAc)_2$ added to complex **1** each time was 2 μL).

Fig. 7. (a) The excitation and emission spectra of complex **3** (5.0×10^{-5} M). (b) Fluorescence spectral changes of complex **1** by the addition of $Sr(OAc)_2$ (5.0×10^{-3} M) ($CHCl_3/CH_3OH$ (1:1), [complex **1**] = 5.0×10^{-5} M, λ_{ex} = 438 nm) (The amount of $Sr(OAc)_2$ added to complex **1** each time was 2 μL)

Fluorescence titration experiments of the alkaline earth metal ions with crystals of complex **1** show the same results in comparison with the UV-Vis titration experiments. The fluorescence intensity of the solution hardly changed after the alkaline earth metal ion was added up to 1 equivalence. The spectroscopic titration clearly indicated that the ratio of the reaction stoichiometry was 1:1. The binding constants of complex **1** upon sequential addition of Ca^{2+}, Sr^{2+} or Ba^{2+} ions were estimated to be 4.71×10^5, 1.92×10^6 and 3.12×10^6 M^{-1}, respectively.

Fig. 8. (a) The excitation and emission spectra of complex **4** (5.0×10^{-5} M). (b) Fluorescence spectral changes of complex **1** by the addition of $Ba(OAc)_2$ (5.0×10^{-3} M) ($CHCl_3/CH_3OH$ = 1:1, *v*/*v*), [complex **1**] = 5.0×10^{-5} M, λ_{ex} = 440 nm) (The amount of $Ba(OAc)_2$ added to complex **1** each time was 2 μL).

Furthermore, complexes **1-4** exhibit strong fluorescence intensities in the solid state at room temperature, as shown in Fig. S6 (a-b). The emission spectra of complexes **1-4** were measured at the appropriate excitation wavelengths of 440 and 420 nm. Complexes **1-4** show maximum emissions at 515.5, 497.5, 490.5 and 532 nm, respectively. The results show that the fluorescence intensity of complex **2** was the strongest among the complexes, and the fluorescence intensity of complexes **3** and **4** were weaker than complex **1**. The differences in the fluorescence intensities could be easily observed in the maximum wavelengths of complexes **1-4**, especially between complexes **3** and **4** which are shifted by 41.5 nm.

According to the obtained experimental data, the differences among the three heterotrinuclear complexes are very obvious and could be utilized in host-guest systems. Also, the complexes with the naphthalene ring show better optical properties.

4. Conclusion

We have designed and synthesized a novel acyclic bis(salamo)-type ligand, H_4L, and obtained the corresponding homotrinuclear Zn(II) complex by the reaction of the bis(salamo)-type tetraoxime ligand H_4L with 3 equivalents of the Zn^{2+} ion. The heterotrinuclear 3d-2s complexes were acquired by the substitution reaction of the homotrinuclear Zn(II) complex with 1 equivalent of $M(OAc)_2$ (M^{2+} = Ca^{2+}, Sr^{2+} or Ba^{2+}). UV-Vis and fluorescence intensity spectral titrations and X-ray crystallography clearly show that the stoichiometry of the homotrinuclear Zn(II) complex is 3:1 (Zn^{2+}/ ligand) and those of the heterotrinuclear complexes are all 2:1:1 (Zn^{2+}/M^{2+}/ligand). The different fluorescence enhancements and maximum wavelength variations of the heterotrinuclear complexes clearly show the success of the transformation from homotrinuclear to heteronuclear complexes, which could be used in host-guest systems. Furthermore, by analyzing the structures of these complexes, the metal-chelate function of the phenoxy oxygen atoms with the M^{2+} ion has stronger coordination than the oxygen atoms of methoxy groups, which may be affected by the electrostatic interaction. The central Zn^{2+} ion of the complex $[Zn_3(L)]^{2+}$ could be replaced by a metal cation that has a suitable size for the cavity. Owing to their electrostatic interaction and size-fit principle, heteronuclear complexes with rare-earth(III) ions may be prepared by substitution reactions, and related research is underway.

Appendix A. Supplementary data

CCDC 1424752, 1424753, 1424754 and 1424755 contain the supplementary crystallographic data for complexes **1**, **2**, **3** and **4**. These data can be obtained free of charge via http://www.ccdc.cam.ac.uk/conts/retrieving.html, or from the Cambridge Crystallographic Data Centre, 12 Union Road, Cambridge CB2 1EZ, UK; fax: (+44) 1223-336-033; or e-mail: deposit@ccdc.cam.ac.uk.

Acknowledgement

This work was supported by the National Natural Science Foundation of China (21361015), which is gratefully acknowledged.

References

[1] (a) H.L. Wu, G.L. Pan, Y.C. Bai, Y.H. Zhang, H. Wang, F.R. Shi, X.L. Wang, J. Kong, J. Photochem. Photobiol. B 135 (2014**)** 33-43;

(b) H.L. Wu, Y.C. Bai, Y.H. Zhang, Z. Li, M.C. Wu, C.Y. Chen, J.W. Zhang, J. Coord. Chem. 67 (2014) 3054-3066;

(c) H.L. Wu, H. Wang, X.L. Wang, G.L. Pan, F.R. Shi, Y.H. Zhang, Y.C. Bai, J. Kong, New J. Chem. 38 (2014) 1052-1061;

(d) H.L. Wu Y.C., Bai, Y.H. Zhang, G.L. Pan, J. Kong, F.R. Shi, X.L. Wang, Z. Anorg. Allg. Chem. 640 (2014) 2062-2071;

(e) H.L. Wu, G.L. Pan, Y.C. Bai, H. Wang, J. Kong, F.R. Shi, Y.H. Zhang, X.L. Wang, Res. Chem. Intermed. 41 (2015) 3375-3388;

(f) H.L. Wu, C.P. Wang, F. Wang, H.P. Peng, H. Zhang, Y.C. Bai, J. Chinese Chem. Soc. 62 (2015) 1028-1034;

(g) C.Y. Chen, J.W. Zhang, Y.H. Zhang, Z.H. Yang, H.L. Wu, G.L. Pan, Y.C. Bai, J. Coord. Chem. 68 (2015) 1054-1071;

(h) H.L. Wu, G.L. Pan, Y.C. Bai, H. Wang, J. Kong, F.R. Shi, Y.H. Zhang, X.L. Wang, J. Chem. Res. 38 (2014) 211-217;

(i) H.L. Wu, G.L. Pan, Y.C. Bai, H. Wang, J. Kong, F.R. Shi, Y.H. Zhang, X.L. Wang, J. Coord. Chem. 66 (2013) 2634-2646.

[2] (a) Y.X. Sun, W.K. Dong, L. Wang, L. Zhao, Y.H. Yang, Chinese J. Inorg. Chem. 25 (2009) 1478-1482;

(b) Y.X. Sun, L. Xu, T.H. Zhao, S.H. Liu, G.H. Liu, X.T. Dong, Synth. React. Inorg. Met. Org. Nano Met. Chem. 43 (2013) 509-513;

(c) Y.X. Sun, X.H. Gao, Synth. React. Inorg. Met. Org. Nano Met. Chem. 41 (2011) 973-978;

(d) Y.X. Sun, S.T. Zhang, Z.L. Ren, X.Y. Dong, L. Wang, Synth. React. Inorg. Met. Org. Nano Met. Chem. 43 (2013) 995-1000;

(e) Y.X. Sun, L. Wang, X.Y. Dong, Z.L. Ren, W.S. Meng, Synth. React. Inorg. Met. Org. Nano Met. Chem. 43 (2013) 599-603;

(f) L. Xu, L.C. Zhu, J.C. Ma, Y. Zhang, J. Zhang, W.K. Dong, Z. Anorg, Allg. Chem. 641 (2015) 2520-2524;

(g) L. Xu, Y.P. Zhang, J.Y. Shi, W.K. Dong, Chinese J. Inorg. Chem. 23 (2007) 1999-2002;

(h) L. Xu, Y.P. Zhang, L. Wang, J.Y. Shi, W.K. Dong, Chinese J. Struct. Chem. 27 (2008) 183-186;

(i) L. Wang, J.C. Ma, W.K. Dong, L.C. Zhu, Y. Zhang, Z. Anorg, Allg. Chem. 642 (2016) 834-839;

(j) X.Y. Dong, Y.X. Sun, L. Wang, L. Li, J. Chem. Res. 36 (2012) 387-390.

[3] (a) X.Q. Song, P.P. Liu, Z.R. Xiao, X. Li, Y.A. Liu, Inorg. Chim. Acta 438 (2015) 232-244;

(b) P.P. Liu, L. Sheng, X.Q. Song, W.Y. Xu, Y.A. Liu, Inorg. Chim. Acta 434 (2015) 252-257;

(c) X.Q. Song, Y.J. Peng, G.Q. Chen, X.R. Wang, P.P. Liu, W.Y. Xu, Inorg. Chim. Acta 427 (2015) 13-21;

(d) X.Q. Song, P.P. Liu, Y.A. Liu, J.J. Zhou, X.L. Wang, Dalton Trans. 45 (2016) 8154-8163;

(e) T.Z. Yu, K. Zhang, Y.L. Zhao, C.H. Yang, H. Zhang, L. Qian, D.W. Fan, W.K. Dong, L.L. Chen, Y.Q. Qiu, Inorg. Chim. Acta 361 (2008) 233-240;

(f) T.Z. Yu, K. Zhang, Y.L. Zhao, C.H. Yang, H. Zhang, D.W. Fan, W.K. Dong, Inorg. Chem. Commun., 10 (2007) 401-403;

(g) T.Z. Yu, W.M. Su, W.L. Li, Z.R. Hong, R.N. Hua, M.T. Li, B. Chu, B. Li, Z.Q. Zhang, Z. Hu, Inorg. Chim. Acta, 359 (2006) 2246-2251;

(h) L.Q. Chai, G. Wang, Y.X. Sun, W.K. Dong, L. Zhao, X.H. Gao, J. Coord. Chem. 65 (2012) 1621-1631.

[4] (a) W.K. Dong, J.C. Ma, L.C. Zhu, Y. Zhang, X.L. Li, Inorg. Chim. Acta 445 (2016) 140-148;

(b) W.K. Dong, J.C. Ma, Y.J. Dong, L.C. Zhu, Y. Zhang, Polyhedron 115 (2016) 228-235;

(c) W.K. Dong, J.G. Duan, Y.H. Guan, J.Y. Shi, C.Y. Zhao, Inorg. Chim. Acta 362 (2009) 1129-1134;

(d) W.K. Dong, J. Zhang, Y. Zhang, N. Li, Inorg. Chim. Acta 444 (2016) 95-102;

(e) W.K. Dong, P.F. Lan, W.M. Zhu, Y. Zhang, J. Coord. Chem. 69 (2016) 1272-1283;

(f) W.K. Dong, J.T. Zhang, Y.J. Dong, Y. Zhang, Z.K. Wang, Z. Anorg, Allg. Chem. 642 (2016) 189-196;

(g) W.K. Dong, F. Zhang, N. Li, L. Xu, Y. Zhang, J. Zhang, L.C. Zhu, Z. Anorg, Allg. Chem. 642 (2016) 532-538;

(h) W.K. Dong, Y.X. Sun, C.Y. Zhao, X.Y. Dong, L. Xu, Polyhedron 29 (2010) 2087-2097;

(i) W.K. Dong, L.S. Zhang, Y.X. Sun, M.M. Zhao, G. Li, X.Y. Dong, Spectrochim. Acta Part A 121 (2014) 324-329;

(j) W.K. Dong, X.N. He, H.B. Yan, Z.W. Lv, X. Chen, C.Y. Zhao, X.L. Tang, Polyhedron 28 (2009) 1419-1428;

(k) J.C. Ma, X.Y. Dong, W.K. Dong, Y. Zhang, L.C. Zhu, J.T. Zhang, J. Coord. Chem. 69 (2016) 149-159.

[5] (a) P. Wang, L. Zhao, Spectrochim. Acta, Part A 135 (2015) 342-350;

(b) P. Wang, L. Zhao, Synth. React. Inorg. Met. Org. Nano Met. Chem. 46 (2016) 1095-1101;

(c) L. Zhao, L. Wang, Y.X. Sun, W.K. Dong, X.L. Tang, X.H. Gao, Synth. React. Inorg. Met. Org. Nano Met. Chem. 42 (2012) 1303-1308;

(d) L. Zhao, X.T. Dang, Q. Chen, J.X. Zhao, L. Wang, Synth. React. Inorg. Met. Org. Nano Met. Chem. 43 (2013) 1241-1246.

[6] S. Akine, T. Nabeshima, Dalton Trans. 47 (2009) 10395-10408.

[7] S.J. Wezenberg, A.W. Kleij, Angew. Chem. Int. Ed. 47 (2008) 2354-2364.

[8] G. Mezei, C.M. Zaleski, V.L. Pecoraro, Chem. Rev. 107 (2007) 4933-5003.

[9] (a) S. Akine, T. Taniguchi, T.J. Nabeshima, Am. Chem. Soc. 128 (2006) 15765-15774;

(b) S. Akine, S. Kagiyama, T. Nabeshima, Inorg. Chem. 46 (2007) 9525-9527;

(c) T. Ohshima, T.I. Wasaki, Y. Maegawa, A. Yoshiyama, K.J. Mashima, Am. Chem. Soc. 130 (2008) 2944-2945.

[10] (a) M.M.J. Smulders, S. Zarra, J.R.J. Nitschke, J. Am. Chem. Soc. 135 (2013) 7039-7046;

(b) N. Kumari, M.A. Hasan, B.D. Ward, L. Mishra, Ind. Eng. Chem. Res. 52 (2013) 15007-15014;

(c) J.P. Costes, F. Dahan, A. Dupuis, Inorg. Chem. 39 (2000) 165-168;

(d) C. Edder, C. Piguet, J.C.G. Bünzli, G. Hopfgartner, Chem. Eur. J. 7 (2001) 3014-3024;

(e) J.C.G. Bünzli, C. Piguet, Chem. Rev. 102 (2002) 1897-1928;

(f) W. Chen, X. Tang, W. Dou, Z. Ju, B. Xu, W. Xu, W. Liu, Chem. Commun. 52 (2016) 5124-5127.

[11] G.W. Gokel, W.M. Leevy, Chem. Rev. 104 (2004) 2723-2750.

[12] (a) T. Nabeshima, S. Akine, Chem. Rec. 8 (2008) 240-251;

(b) T. Nabeshima, Bull. Chem. Soc. Jpn. 83 (2010) 969–991; (c) T. Nabeshima, S. Akine, C. Ikeda, M. Yamamura, Chem. Lett. 39 (2010) 10-16;

(d) G. Lautrette, B. Kauffmann, Y. Ferrand, C. Aube, N. Chandramouli, D. Dubreuil, I. Huc, Angew. Chem. Int. Ed. 52 (2013) 11517-11520.

[13] (a) E. Barreiro, J.S. Casas, M.D. Couce, A. Sánchez, J. Sordo, E. M. Vázquez-López, J. Inorg. Biochem. 131 (2014) 68-75;

(b) G. Brewer, L.J. Alvarado, S. Lear, C. Viragh, P.Y. Zavalij, Inorg. Chim. Acta 439 (2016) 111-116;

(c) E.S. Bazhina, G.G. Aleksandrov, N.N. Efimov, E.A. Ugolkova, V. Minin, A. Sidorov, V. Novotortsev, I. Eremenko, Rus. Chem. Bul. 62 (2013) 962-965;

(d) P. Guerriero, S. Tarnburini, P.A. Vigato, Coord. Chem. Rev. 139 (1995) 17-243;

(e) P. Totaro, K.C.M. Westrup, M.E. Boulon, G.G. Nunes, D.F. Back, A. Barison, S. Ciattini, M. Mannini, L. Sorace, J.F. Soares, Dalton Trans. 42 (2013) 4416-4426.

[14] Y. Nakamura, M. Yonemura, K. Arimura, N. Usuki, M. Ohba, H. Okawa, Inorg. Chem. 40 (2001) 3739-3744.

[15] M. Yonemura, K. Arimura, K. Inoue, N. Usuki, M. Ohba, H. Okawa, Inorg. Chem. 41 (2002) 582-589.

[16] L.K. Das, A. Biswas, C.J. Gómez-García, M.G. Drew, A. Ghosh, Inorg. Chem. 53 (2013) 434-445.

[17] (a) A. Kumar, R. Pandey, R.K. Gupta, V. Mishra, S.M. Mobin, D.S. Pandey, Dalton Trans. 43 (2014) 6365-6376;

(b) S. Akine, T. Taniguchi, T. Nabeshima, Chem. Lett 7 (2001) 682-683; (c) S. Ghosh, S. Biswas, A. Bauzá, M. Barceló-Oliver, A. Frontera, A. Ghosh, Inorg. Chem. 52 (2013) 7508-7523.

[18] (a) W.K. Dong, J.C. Ma, L.C. Zhu, Y. Zhang, Cryst. Growth Des. 16 (2016) 6903-6914;

(b) W.K. Dong, X.L. Li, L. Wang, Y. Zhang, Y.J. Ding, Sens. Actuators. B 229 (2016) 370-378;

(c) W.K. Dong, F.A. Sunday, Y. Zhang, Y.X. Sun, X.Y. Dong, Sens. Actuators. B 238 (2017) 727-734;

(d) W.K. Dong, J.C. Ma, L.C. Zhu, Y. Zhang, New J. Chem. 40 (2016) 6998-7010;

(e) S.T. Zhang, T.R. Li, B.D. Wang, Z.Y. Yang, J. Liu, Z.Y. Wang, W.K. Dong, Dalton Trans. 43 (2014) 2713-2717.

[19] (a) S. Akine, S. Sairenji, T. Taniguchi, T. Nabeshima, J. Am. Chem. Soc. 135 (2013) 12948-12951;

(b) A.J. Gallant, M. Yun, M. Sauer, C.S. Yeung, M. MacLachlan, J. Org. Lett. 7 (2005)

4827-4830;

(c) H.A. Tran, J. Collins, P.E. Georghiou, New J. Chem. 32 (2008) 1175-1182;

(d) S. Akine, T. Tadokoro, T. Nabeshima, Inorg. Chem. 51 (2012) 11478-11486.

[20] A.W. Addison, T.N. Rao, J. Reedijk, J.V. Rijn, G.C. Verschoor, J. Chem. Soc. Dalton Trans. 7 (1984) 1349-1356.

[21] A. Majumder, G.M. Rosair, A. Mallick, N. Chattopadhyay, S. Mitra, Polyhedron 25 (2006) 1753-1762.

[22] (a) J. Cheng, X. Ma, Y. Zhang, J. Liu, X. Zhou, H. Xiang, Inorg. Chem. 53 (2014) 3210-3219;

(b) Q.H. Meng, P. Zhou, F. Song, Y.B. Wang, G.I. Liu, H. Li, Cryst. Eng. Comm. 15 (2013) 2786-2790;

(c) C.E. Burrow, T.J. Burchell, P.H. Lin, F. Habib, W. Wernsdorfer, R. Clérac, M. Murugesu, Inorg. Chem. 48 (2009) 8051-8053.

Table 1

Crystallographic data and refinement parameters for the complexes **1**, **2**, **3** and **4**.

Complex	**1**	**2**	**3**	**4**
Empirical formula	$C_{41}H_{45}Cl_9N_4O_{16}Zn_3$	$C_{37}H_{35}CaCl_3N_4O_{14}Zn_2$	$C_{36}H_{34}N_4O_{14}SrZn_2$	$C_{39}H_{43}BaCl_3N_4O_{16}Zn_2$
Formula weight	1364.97	1036.86	965.03	1198.20
T (K)	173.00(10)	293(2)	294.29(10)	291.73(10)
Wavelength (Å)	0.71073	0.71073	0.71073	0.71073
Crystal system	monoclinic	triclinic	triclinic	triclinic
Space group	$P2_1/n$	$\bar{P}1$	$\bar{P}1$	$\bar{P}1$
a (Å)	14.0480(4)	13.4794(7)	12.6197(14)	10.6854(5)
b (Å)	16.5494(3)	13.6682(6)	13.346(2)	14.1383(7)
c (Å)	23.6735(5)	15.4156(9)	15.6864(18)	16.2738(13)
α (°)	90	85.483(4)	114.099(13)	73.657(6)
β (°)	100.464(2)	65.228(5)	104.696(10)	88.178(5)
γ (°)	90	65.053(5)	99.435(11)	78.971(4)
V (Å^3)	5412.2(2)	2321.6(2)	2223.2(6)	2315.0(2)
Z	4	2	2	2
D_{calc} (g cm^{-3})	1.675	1.483	1.442	1.719
Absorption coefficient (mm^{-1})	1.831	1.381	2.329	2.115
θ range for data collection (°)	3.377-26.021	3.40-26.02	3.409-26.020	3.290-26.022
F(000)	2760.0	1056.0	976.0	1200
h/k/l (minimum, maximum)	–13, 17/–20, 19/–29, 23	–15, 16/–16, 16/–19, 18	–14, 15/–16, 13/–17, 19	–13, 12/–16, 17/–17, 20
Crystal size (mm)	0.21 × 0.24 × 0.32	0.25 × 0.27 × 0.31	0.17 × 0.18 × 0.23	0.21 × 0.23 × 0.25
Reflections collected	23279/10650 [R_{int} = 0.049]	17514/9119 [R_{int}= 0.043]	15027/8714 [R_{int}= 0.079]	16597/9101 [R_{int}= 0.032]
Independent reflection	10650	9119	8714	9101
Completeness to 26.32 (%)	99.71	99.76	99.75	99.79
Data/restraints/parameters	10650/0/670	9119/0/554	8714/0/518	9101/0/596
Final R indices [I > 2σ (I)]	R_1 = 0.0519, wR_2 =0.1136	R_1 = 0.0524, wR_2 =0.1549	R_1 = 0.0690, wR_2 =0.0926	R_1 = 0.0520, wR_2 =0.1453
R indices (all data)	R_1 = 0.0812, wR_2 =0.0968	R_1 = 0.0731, wR_2 =0.1377	R_1 = 0.0963, wR_2 =0.1139	R_1 = 0.0695, wR_2 =0.1286
Goodness-of-fit for (F^2)	1.032	1.048	1.025	1.050
Largest difference peak and hole (e Å^{-3})	0.91, –1.10	0.72, –0.65	1.06, –0.61	1.99, –1.08

a. $R_1 = \Sigma||F_o| - |F_c||/\Sigma|F_o|$; b. $wR_2 = [\Sigma w(F_o^2 - F_c^2)^2/\Sigma w(F_o^2)^2]^{1/2}$, $w = [\sigma^2(F_o^2) + (0.0784P)^2 + 1.3233P]^{-1}$, where $P = (F_o^2 + 2F_c^2)/3$; c. GOF = $[\Sigma w(F_o^2 - F_c^2)^2/n_{obs} - n_{param})]^{1/2}$;

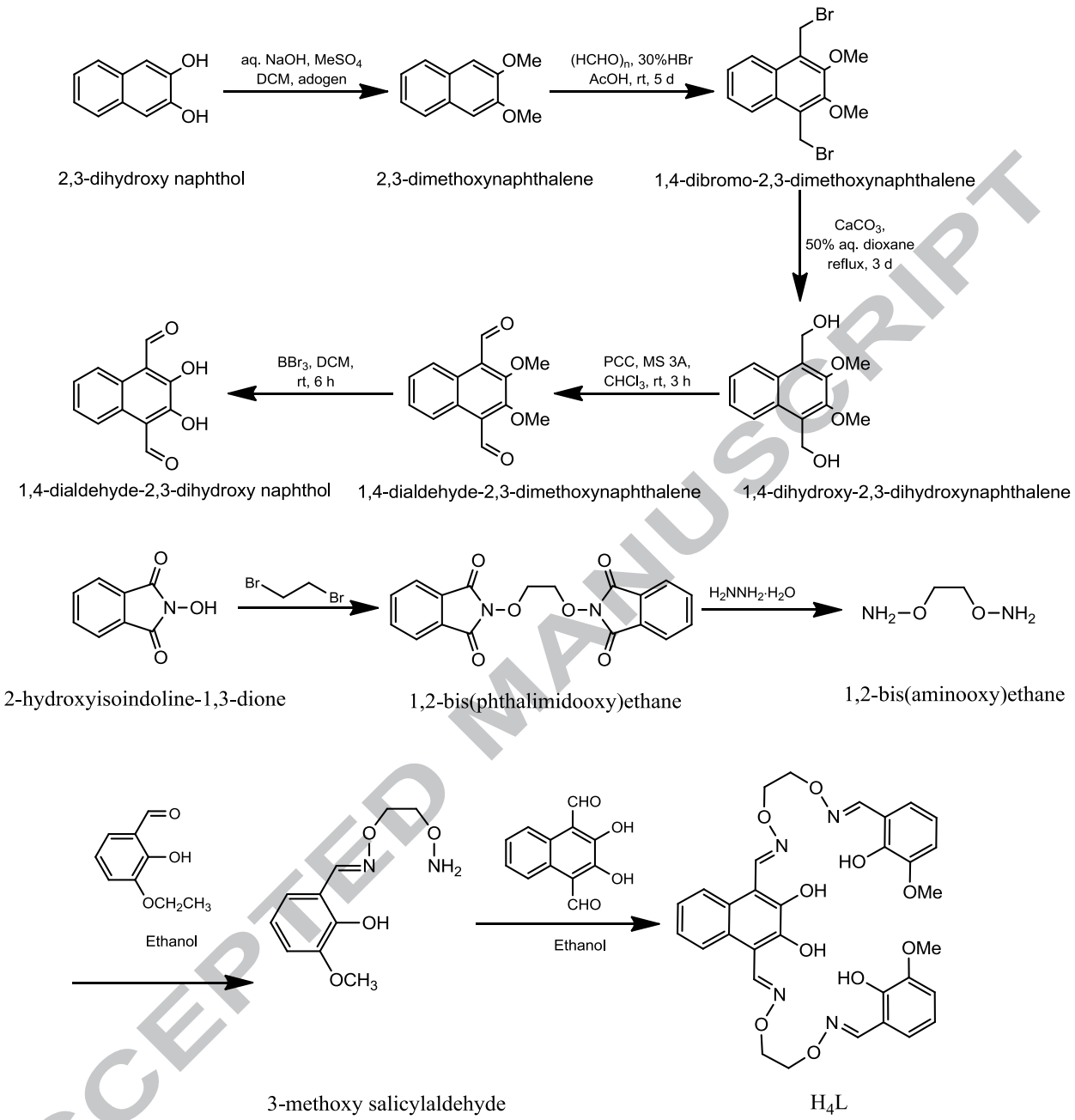

Scheme 1

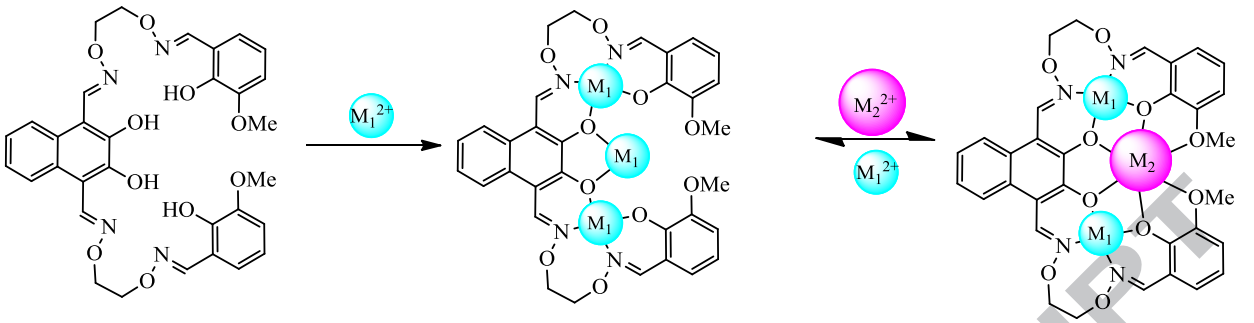

H_4L Homotrinuclear complex Heterotrinuclear complex

M_1=Zn; M_2=Ca, Sr, Ba.

Scheme 2

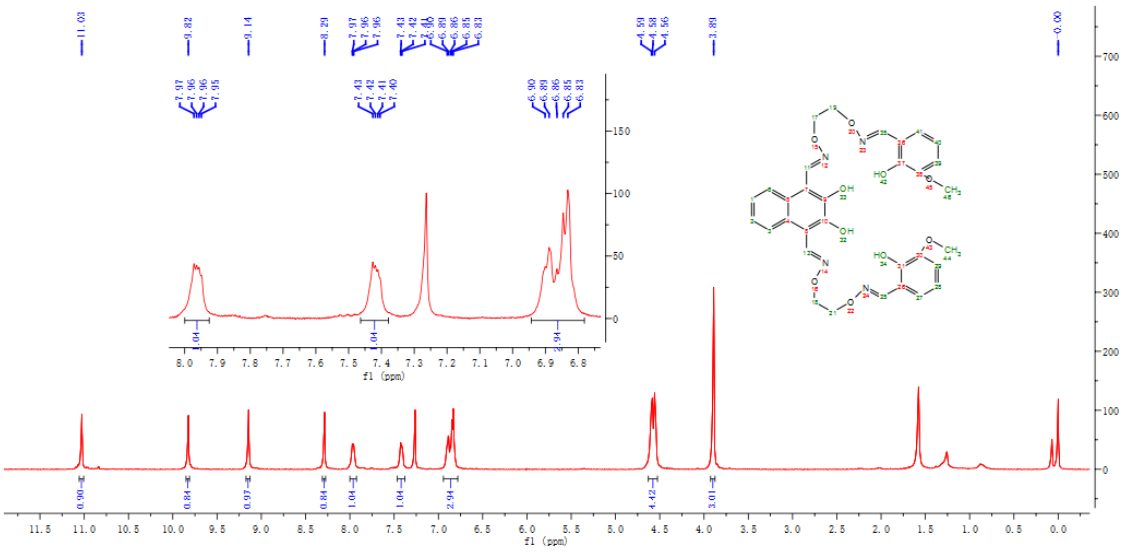

^{1}H NMR (400 MHz, $CDCl_3$) δ 11.03 (s, 2H), 9.82 (s, 2H), 9.14 (s, 2H), 8.29 (s, 2H), 7.97 (q, J = 3.2 Hz, 2H), 7.41 (q, J = 6.0, 2.9 Hz, 2H), 7.06 – 6.68 (m, 6H), 4.58 (t, 8H), 3.89 (s, 6H).

Fig. 1.

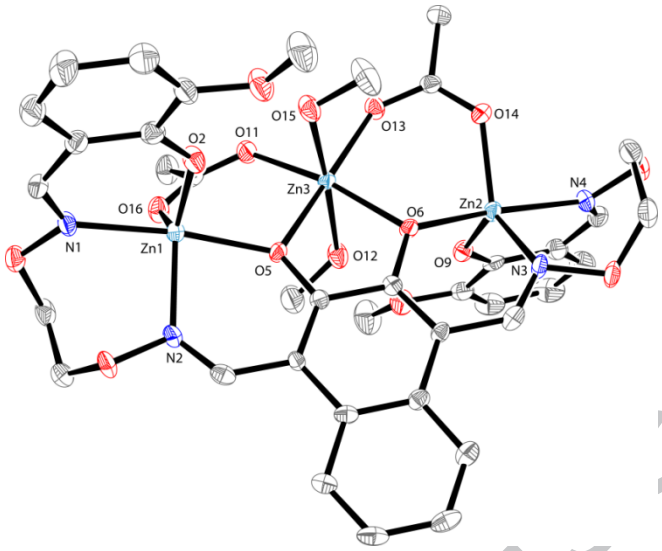

Fig. 2.

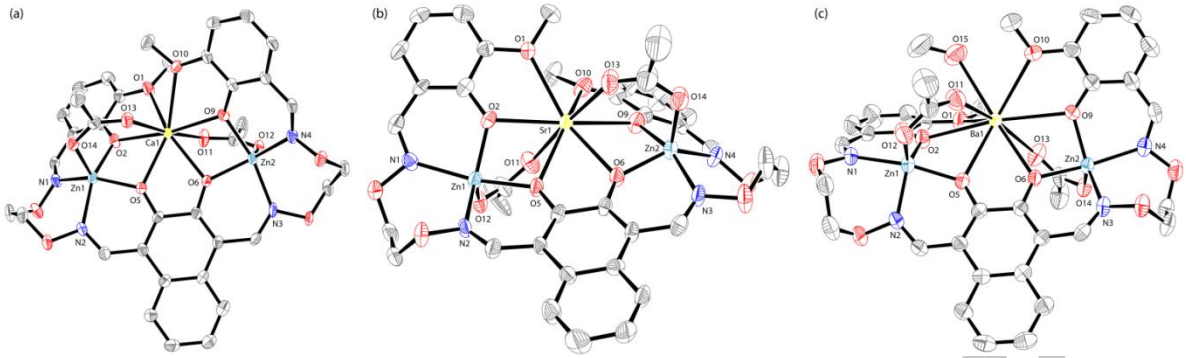

Fig. 3.

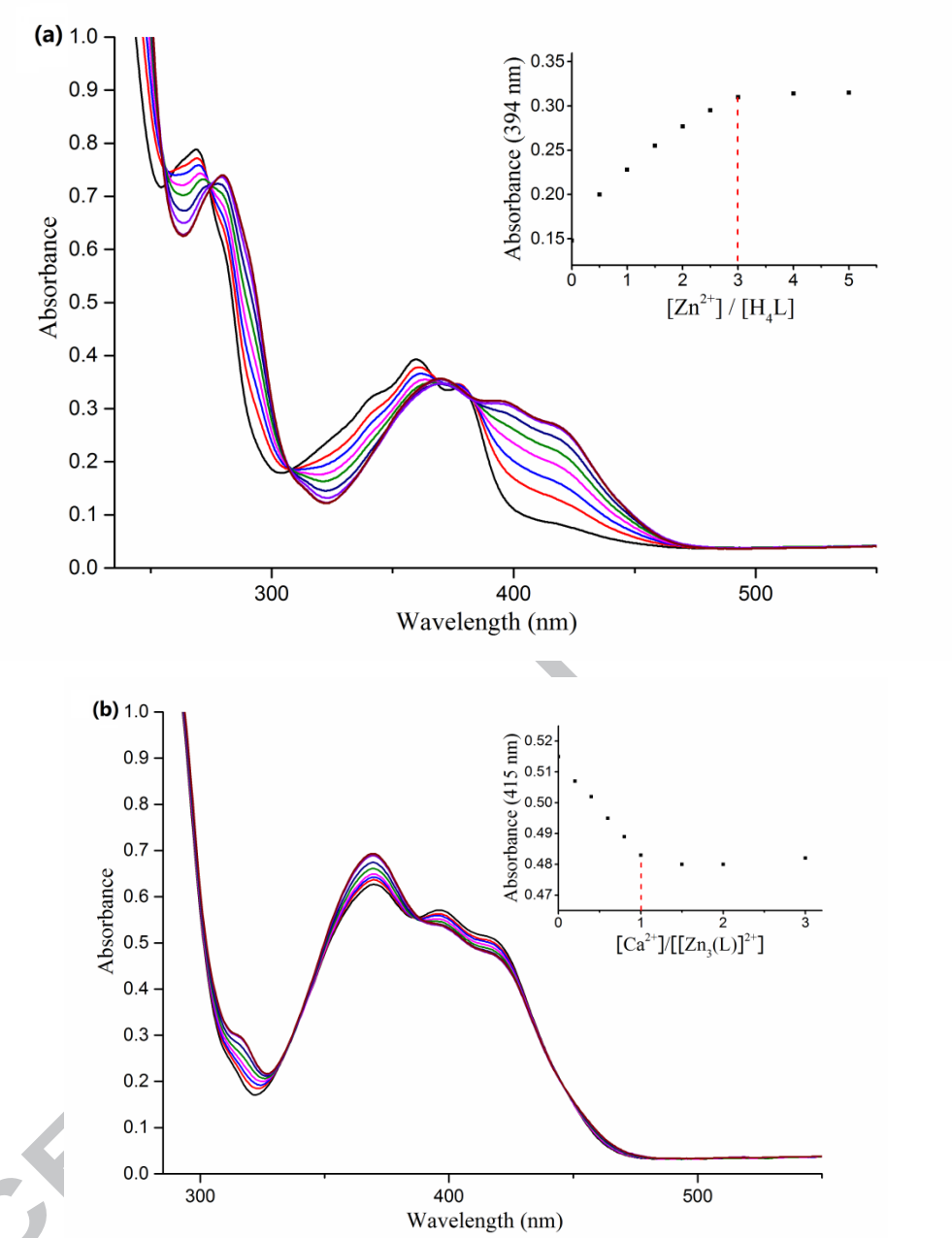

Fig. 4.

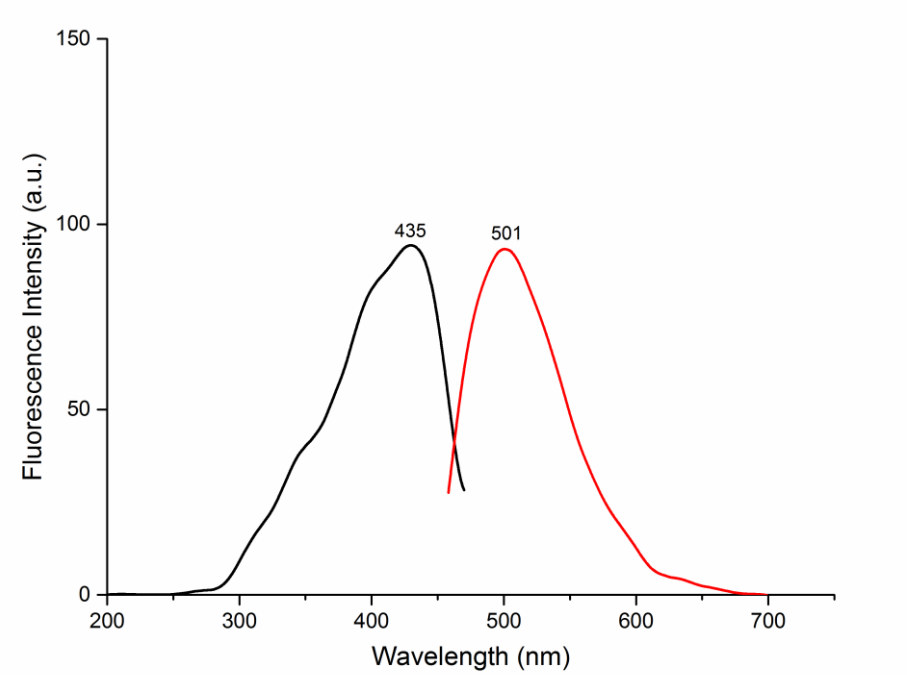

Fig. 5.

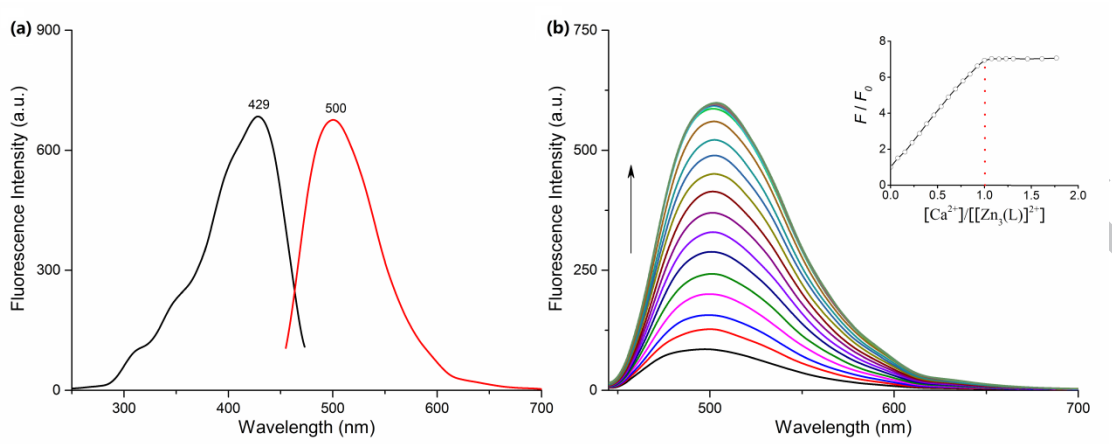

Fig. 6.

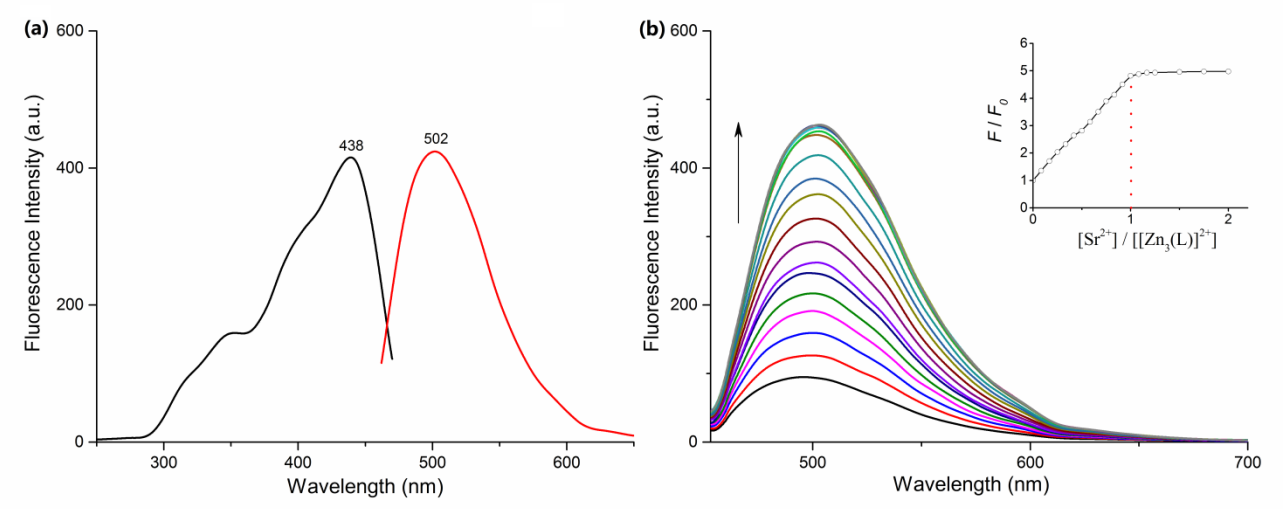

Fig. 7.

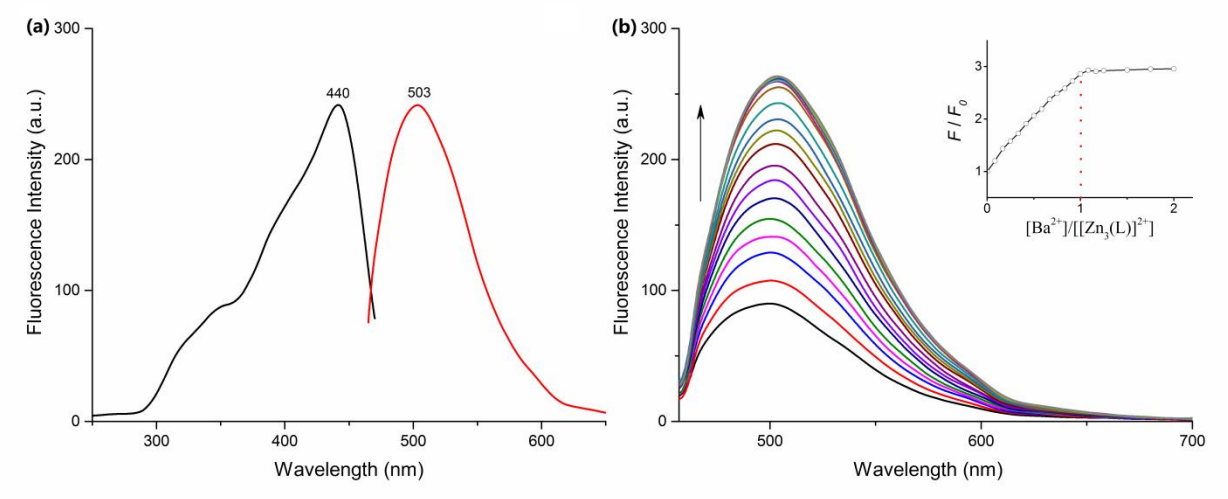

Fig. 8.